KSCE Journal of Civil Engineering 29 (2025) 100005

Contents lists available at ScienceDirect

KSCE Journal of Civil Engineering

journal homepage: www.elsevier.com/locate/kscej

A BIM and AR-based indoor navigation system for pedestrians on smartphones

Wensheng Zhang [a], Yanjing Li [a], Pengcheng Li [b], Zhenan Feng [c,*]

[a] School of Traffic and Transportation, Shijiazhuang Tiedao University, Shijiazhuang 050043, PR China
[b] Hebei Traffic Investment Intelligent Technology Co. LTD, Shijiazhuang 050000, PR China
[c] School of Built Environment, Massey University, Auckland 0632, New Zealand

ARTICLE INFO

Keywords:
Indoor navigation
BIM
AR
Network construction
Navigation algorithm

ABSTRACT

Indoor navigation technology, as an emerging location information service, has shown continuous growth in its application demand in recent years. In indoor navigation, indoor localization and path planning are the key factors affecting navigation quality. Most of the existing methods rely on traditional methods for indoor localization with high implementation costs. As for path planning, most methods lack the acquisition and use of semantic information, affecting navigation's practicality and intuitiveness. To alleviate the above problems, we propose a building information modeling (BIM) and augmented reality (AR)-based indoor navigation system for pedestrians that can be implemented on smartphones. Specifically, we first map a three-dimensional model space subdivided by a triangular prism to the two-dimensional plane in order to construct an indoor navigation network. Secondly, the information is analyzed using inertial navigation system technology to identify indoor positions. Then, we propose an indoor augmented reality navigation algorithm based on architectural and spatial information (IARA) algorithm for indoor path planning. Finally, we integrated the above technologies and built an indoor pedestrian navigation system based on BIM and AR technologies. Experiments in specific scenarios show that our system ensures navigation stability while obtaining results that are more relevant to the needs of pedestrians.

1. Introduction

As the number of complex buildings (like shopping centers, airports, and hospitals) continues to surge, the challenge of precisely determining indoor positions and offering navigation solutions has become increasingly significant (El-Sheimy & Li, 2021). These complex and multi-level buildings demand innovative solutions for accurate positioning and guidance as global navigation satellite systems (e.g., GPS) are usually inaccessible indoors (Blunck, Godsk & Grønbæk, 2010). An indoor navigation system can be a valuable tool for building users in normal as well as emergency situations (Lovreglio & Kinateder, 2020; Bernardini, Lovreglio & Quagliarini, 2023). Advances in technologies such as Building Information Modeling (BIM), Augmented Reality (AR), and Artificial Intelligence (AI) are avenues for innovative approaches to indoor navigation systems (Teo & Cho, 2016; Wang, 2019; Grejner-Brzezinska, Toth & Markiel, 2009).

For indoor navigation, research is currently carried out in the directions of indoor positioning, path planning, and navigation display. Among them, indoor positioning technology either relies on traditional algorithms for position solving, such as TOA/TDOA time-based and AOA/AOD angle-based measurements or relies on base stations or sensors for fusion positioning, which is more complex and costly. Indoor path planning, on the other hand, is mostly based on mobile robots, relying on 2D architectural drawings, using topological data information, and selecting optimal paths by improving algorithms such as A* and ACOA, which have high utilization of indoor building geometries but lack access to and use of semantic information. Meanwhile, the practicality and intuitiveness of navigation at the two-dimensional level are affected. The use of new-generation information technologies such as BIM and AR can provide effective technical means for model data acquisition and spatial positioning perception for indoor positioning and path planning, offering users a practical and technological indoor navigation experience.

Several methods have been investigated for indoor navigation. Traditional sensor- and signal-based indoor positioning methods (e.g., WiFi, LiFi, Bluetooth, or RFID) do not take into account the complexity of the indoor environment and its interference with the positioning signals when implementing indoor navigation (Zafari, Gkelias & Leung, 2019; van Bommel & van Bommel, 2019; He & Chan, 2015). In addition, how to balance the cost of installing indoor devices and adjusting the po-

* Corresponding author.
E-mail addresses: zws@stdu.edu.cn (W. Zhang), z.feng1@massey.ac.nz (Z. Feng).

https://doi.org/10.1016/j.kscej.2024.100005
Received 16 February 2024; Received in revised form 10 June 2024; Accepted 20 July 2024

sition of signaling devices due to changes in the indoor environment are also difficult aspects of the indoor navigation problem (Harle, 2013; Yassin, Nasser & Awad, 2016). Therefore, it is crucial to establish appropriate infrastructure for signal transmission and reading to ensure optimal performance. Both BIM and AR can play a key role in overcoming these existing challenges.

BIM is a digital modeling and information management technology that contains a variety of model information throughout the life cycle of an engineering project, which can provide data model support for indoor navigation (Sacks, Eastam, Lee & Teichloz, 2018). As such, the comprehensive and detailed information offered by BIM makes it possible to facilitate indoor positioning tasks. AR is a cutting-edge technology that fuses virtual information with the real world, applying computer-generated information such as text and three-dimensional models after simulation of simulation to the real world to achieve "augmentation" (Milgram & Kishino, 1994). Its substantive core contains a variety of technologies, such as visual positioning, 3D modeling, real-time tracking, and registration, which can provide auxiliary positioning support for indoor navigation (Kim & Jun 2008). Integrating BIM and AR technology for indoor positioning can overcome several existing navigation challenges, such as signal interference and equipment costs, and can minimize the influence of the multipath effect, signal attenuation, and Doppler effect on positioning accuracy. Finally, BIM and AR have the potential to provide users with accurate navigation path guidance and realistic navigation experience on devices they are familiar with, such as smartphones.

In this paper, we propose an indoor navigation system for pedestrians that runs on a smartphone. Specifically, we carry out research on the method and application of indoor navigation using BIM technology. By parsing the IFC standard model, which contains complete data, we can obtain the geometric information for the walls, doors, and passages in the indoor space. Also, we can store the semantic information of the nodes, which can be used as a source of information data for indoor navigation. By integrating with AR technology, we can provide the mapping information data of the AR-labeled nodes to establish the indoor navigation road network to achieve node matching, thus completing indoor positioning. The system can also be used for path planning through the IARA algorithm, thus providing technical support for indoor navigation.

The contributions of this paper are summarized as follows:

(1) We construct an indoor navigation road network based on BIM and AR technology.
(2) We design an indoor positioning method based on BIM and AR technology.
(3) We propose the IARA algorithm and validate it in a real-world environment.
(4) We built and applied an indoor navigation system based on BIM and AR technology. The application results show that the indoor navigation method based on BIM and AR technology proposed in the paper is correct and feasible.

2. Related works

2.1. Indoor network reconstruction

The first category of related research involves the construction of indoor road networks, which encompasses considerations such as architectural entities, spatial layouts, and topological structures (Li, Cao & Li, 2022). These networks are supported by various data sources, which can be categorized into location data, two-dimensional (2D) floor plan data, and three-dimensional (3D) model data (Morar, Moldoveanu & Mocanu, 2020). 2D-floor plan data simplifies indoor representations but lacks elevation information necessary for complex building structures, such as floor connections and obstacles (Li, Men & Mao, 2023). Conversely, 3D building models offer detailed information, including vertical obstacles, floor height differences, and emergency exits (Fu, Zhang & Wang, 2021). However, acquiring sensor data for such models must consider equipment costs and challenges associated with incomplete area coverage and high pedestrian freedom of movement.

In terms of building a planar pedestrian network, Zhou et al. (Zhou, Zheng & Huang, 2020) used an indoor and outdoor integrated pedestrian road network through crowdsourced track data recorded by positioning sensors and inertial sensors of smartphones. Liu et al. (Liu & Sun, 2012) used two-dimensional laser scanning data obtained in real time to construct an all-round plane map of the indoor environment and complete the autonomous positioning.

In emergencies within large buildings, the two-dimensional layout and emergency exits may be insufficiently clear compared to three-dimensional models, which offer crucial building information. To address this, Nikoohemat et al. (Nikoohemat, Diakité & Zlatanova, 2020) proposed a rapid and automated 3D building reconstruction scheme, enabling multi-layer navigation path planning. Ochmann et al. (Ochmann, Vock & Wessel, 2016) introduced a method for automatically extracting geometric information from buildings and reconstructing parametric 3D models using indoor point cloud data. Macher et al. (Macher, Landes & Grussenmeyer, 2017) presented a semi-automatic approach for indoor 3D reconstruction of existing buildings based on point clouds, enhancing model accuracy and reliability. Liu et al. (Liu, Luo & Hou, 2020) extracted and classified building structural information to generate 3D indoor map models using BIM models and deep learning, enabling indoor mobile positioning and navigation functionalities. Li et al. (Li, Zhang & Pan, 2022) integrated 3D geometric modeling with connection attributes and semantic elements of space, extending the IndoorGML standard navigation module and introducing semantic information for indoor spaces, thus proposing an indoor navigation model. Jamali et al. (Jamali, Abdul-Rahman & Boguslawski, 2017) explored a three-dimensional automatic modeling method for indoor navigation networks based on geometric models of indoor environments. Xu et al. (Xu, Wei & Zlatanova, 2017) utilized BIM (IFC) data to extract geometric and semantic information, constructing indoor navigation networks using two-dimensional and three-dimensional spatial subdivision methods to facilitate path planning considering obstacles and addressing limitations of two-dimensional plan-based methods that overlook rich semantic information of building components.

The comparison between two-dimensional planar data and three-dimensional model data highlights the richer spatial characteristics and semantic information provided by the latter, typically represented by CityGML, IFC, and IndoorGML (Alattas, Zlatanova & van Oosterom, 2017; Kim, Yoo & Li, 2014) (Table 1). CityGML is commonly utilized for visualizing 3D city model data and conducting basic spatial analyses. IndoorGML focuses on building information crucial for intelligent robot navigation, albeit with a limited expression of attribute information for indoor space objects and obstacles. On the other hand, IFC primarily serves the management of various information during architectural design and planning, offering comprehensive definitions and classifications for interior element types and their relationships.

In this study, the primary framework revolves around a two-dimensional indoor navigation network, with three-dimensional navigable free space information translated onto a two-dimensional plane. This approach enables the fusion of two-dimensional and three-dimensional data for constructing an indoor road network.

2.2. Indoor pedestrian positioning

The second category of related research focuses on the indoor positioning of pedestrians. Due to signal loss and poor propagation of global satellite navigation systems indoors, current indoor positioning relies mainly on technologies like WiFi, ultra-wideband (UWB), radio frequency identification (RFID), geomagnetic positioning, Bluetooth, and LiFi (Bargh & de Groote, 2008; Mazhar, Khan & Sällberg, 2017; Rizk, Elmogy & Yamaguchi, 2022; Riady & Kusuma, 2022; Hu, Liao & Lu, 2016;

Table 1
Comparison of spatial data models.

	CityGML	IndoorGML	BIM (IFC based)
Application Scenarios	Visual display	Robotics navigation	Architectural design, information management
Geometric forms	Two-dimensional boundary, three-dimensional entity	Two-dimensional boundary, three-dimensional entity	Two-dimensional boundary, three-dimensional entity
Semantic Information	Appearance, function	Symbols	Location, Connectivity, Properties
Topology	Topological objects	Topology Nodes	Topological objects, nodes

Haas, Yin, Wang & Chen, 2016). However, Bluetooth and WiFi signals are susceptible to indoor environmental interference, while RFID and ultrasound-based methods require placing numerous devices indoors, leading to higher navigation costs (Topak, Pekericli & Tanyer, 2018; Agrawal & Singh, 2014; Subedi & Pyun, 2020).

To address these challenges, researchers have combined multiple technologies such as UWB with inertial navigation, WiFi with inertial navigation, and GPS, RFID, WiFi, and pedometers to enhance indoor positioning. Riady et al. (Riady & Kusuma, 2022) proposed an indoor positioning method that merges low-power Bluetooth fingerprinting with pedestrian dead reckoning. Hu et al. (Hu, Liao & Lu, 2016) integrated fingerprint positioning with time positioning, introducing a deep learning-based hybrid indoor positioning system with superior accuracy compared to fingerprint-based and distance-based polygonal positioning techniques by 267 % and 496 %, respectively.

Smartphone devices indeed offer a comprehensive array of sensors, including WiFi and Bluetooth modules, accelerometers, gyroscopes, magnetometers, and cameras, making them ideal for indoor pedestrian positioning. Several studies have leveraged smartphones for this purpose. For example, Dong et al. (Dong & Xiao, 2015) introduced a method utilizing smartphone cameras and sensors for indoor positioning and navigation, achieving an average positioning time of 3.85 s, with a positioning error of <2 m and an orientation error of <6°. Serra et al. (Serra, Carboni & Marotto, 2010) achieved indoor positioning through dead reckoning combined with 2D barcodes, accelerometer, and magnetometer data. Ta (Ta, 2017) fused various sensor information, such as WiFi and Bluetooth signals, with inertial sensors for accurate indoor positioning, albeit with a requirement for real-time monitoring of users' step length and frequency, potentially impacting smartphone battery life due to computational and energy consumption. Chen et al. (Chen, Zhu & Jiang, 2015) proposed an indoor positioning framework combining smartphone sensors with iBeacons to correct pedestrian dead reckoning bias, demonstrating significant improvements in positioning accuracy and robustness against initial point estimation errors in experimental results.

Indeed, various studies have explored augmented reality (AR) solutions for indoor pedestrian positioning. De et al. (de Oliveira, Andrade & de Oliveira, 2017) utilized mobile AR and beacon technology to assist wheelchair users in safe indoor navigation, offering features like identifying optimal routes to avoid obstacles and slopes. Yan et al. (Yan, Liu & Cui, 2015) introduced an indoor navigation strategy merging WiFi positioning with mobile AR on the Android platform, demonstrating high accuracy and real-time performance. Bai et al. (Bai, Huang & Prasad, 2019) reviewed indoor positioning methods leveraging deep learning for image-based localization and sensor fusion incorporating image data. Hsieh et al. (Hsieh, Chen & Nien, 2019) proposed an acoustic indoor positioning approach using AI and Building Information Modeling (BIM), employing Virtual Reality (VR) and Head-Related Transfer Function (HRTF) technology to simulate virtual sound fields, achieving a room area prediction accuracy of approximately 90 % with deep learning models. Park et al. (Park, Cho & Martinez, 2016) integrated BIM-based path planning with various positioning technologies for an indoor navigation system for autonomous mobile robots, highlighting the utility of both BIM and AR technologies in addressing indoor navigation challenges.

2.3. Navigation path optimization

The third category of related research delves into indoor navigation path optimization algorithms, encompassing genetic algorithm-based, deep learning-based, and particle swarm optimization-based methods. Yan et al. (Yan, Zlatanova & Lee, 2021) addressed indoor navigation path challenges using Dijkstra and B&B algorithms with QR code indoor positioning, applicable to museum or hospital navigation. Xu et al. (Xu, Wen & Zhang, 2015) proposed a pedestrian shortest path planning scheme based on the Dijkstra algorithm, incorporating path smoothing and user preference analysis for personalized navigation. Alqahtani et al. (Alqahtani, Alshamrani & Syed, 2018) reviewed indoor navigation systems, comparing various shortest-path algorithms and techniques across multiple sensor environments. Some studies also optimize paths for energy efficiency, user preferences, or minimal turns, such as Pala et al. (Pala, Osati & López-Colino, 2013) with the HCTNav algorithm, validated for lower memory usage compared to Dijkstra's algorithm. Li et al. (Li, Park & Shin, 2017) tailored a shortest-path planning algorithm for dynamic indoor environments based on multi-access point topology analysis. Zhou et al. (Zhou, Chen & Huang, 2018) proposed an environmentally conscious optimal indoor path planning method, enhancing user experience by integrating navigation cost functions and environmental semantics into Dijkstra's algorithm. While previous studies have focused on route optimization and cost reduction of sensor devices, the indoor navigation approach proposed in this paper prioritizes the need for pedestrians to ensure accurate location confirmation, obtain clear directions, and satisfy their interest in surrounding amenities and services in indoor navigation without the need for additional hardware.

3. The proposed indoor navigation system

This study proposes an indoor navigation system using BIM and AR technologies. As shown in Fig. 1, this system mainly includes three modules: indoor navigation network construction, indoor positioning, and an indoor navigation path optimization algorithm.

First of all, the two-dimensional indoor navigation network is taken as the main framework, and according to the BIM data of the building, the three-dimensional navigable spatial information is mapped to the two-dimensional plane. The two-dimensional and three-dimensional data are then fused to realize the construction of the indoor network. Secondly, based on visual and inertial navigation, the AR marker node library with a known position is introduced. AR nodes are special signs or patterns placed in an indoor environment that contain location information such as direction, distance, and location name. We use computer vision to detect AR nodes and obtain node information. AR nodes are placed according to the selection rules of AR nodes, and through camera calibration and coordinate system transformation, node matching is completed to achieve indoor positioning. Finally, an indoor augmented reality navigation algorithm based on architectural and spatial information (IARA algorithm) is proposed. The algorithm combines several optimization parameters, such as the number of AR marker nodes, utilization rate, and path distance, and establishes a multi-objective path optimization model to provide pedestrians with indoor navigation services with route planning, location confirmation, direction guidance, and surrounding information to meet individual needs.

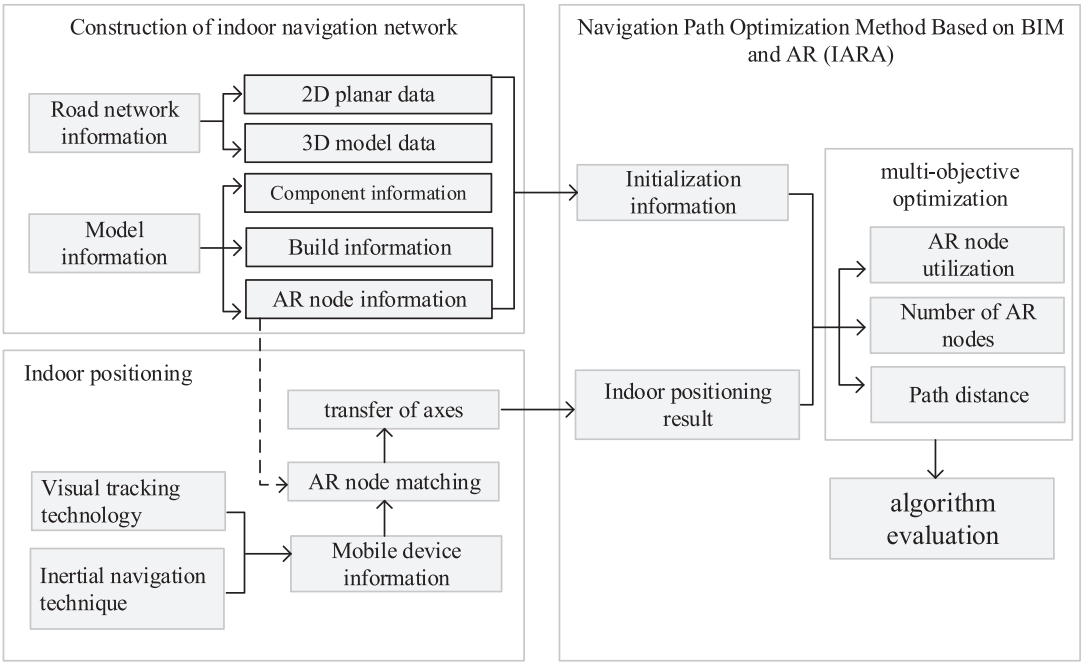

Fig. 1. Diagram of the indoor navigation method.

3.1. Indoor navigation graph construction

The IFC standard, recognized internationally in building information modeling, defines and organizes numerous interior element types and their inheritance relations, offering rich contextual data for indoor navigation road network construction (Laakso & Kiviniemi, 2012). Leveraging this standard, this paper undertakes the extraction and classification of component information, establishing associative mechanisms, and facilitating the extraction and storage of spatial features and semantic data within BIM model datasets.

While 3D maps furnish comprehensive spatial insights, encompassing building structures and room layouts for enhanced spatial perception, 2D indoor navigation networks provide straightforward plane-based navigation data. By converting 3D free navigation spatial data into a plane navigation network and combining it with building data and AR node information, the seamless integration of 3D maps and 2D indoor navigation networks is realized. Users can effortlessly switch between various views to access the desired navigation and positioning information.

When using the rule-based grid method to divide two-dimensional plane data, it is necessary to consider the height characteristics of obstacles and AR nodes as well as the semantic processing of three-dimensional model information. Therefore, this paper adopts the classification and inheritance relationship of building component information outlined in the IFC standard model and classifies and inherits the building component information according to the IFC standard model, including panels, walls, doors, floors, columns, windows, beams, stairs, building floors, public corridors, and other elements.

The geometric and semantic data extracted and stored according to IFC standards are translated onto a plane, where the size of building spaces is determined by the indoor floor length in IFC data. Grids are then applied to divide the floor, with the initial points serving as guide points and their values adjusted based on building node information and AR node selection criteria. Utilizing the topological mapping of data from the IFC standard model onto the floor plan, the IsLocked attribute in the IFC parameters discerns whether revolving doors are locked during element projection. If the IsLocked property is set to true, it indicates that the gate is locked and pedestrians cannot pass through, and the corresponding grid value is set to a value of 0. If the IsLocked property is set to false, it indicates that the gate is unlocked and pedestrians can pass through, and the grid value is set to 1. The IsARPoint property is used to identify nodes. Similarly, the Grid value is set to 0 when Door A is closed, and the Grid value is set to 1 when Door B is open. Geometric information such as walls (IfcWall), columns (IfcColumn), doors (IfcDoor), and furnishings (IfcFurnishingElement) are mapped to the 2D grid as obstacles, with grid values set to 0. Taking Shijiazhuang Metro Plaza as an example, illustrated in Fig. 2, in a partial floor plan of the metro plaza, there are two gates labeled A and B. Gate A is currently locked with its IsLocked property set to true, while Gate B is unlocked with its property set to false. After mapping the build information to a two-dimensional grid, it can be shown in Fig. 3.

The indoor navigation process needs to consider spatial elements such as obstacles and AR nodes. Obstacles have a certain height. In order to facilitate pedestrians to see them, AR nodes are placed at a certain height on the ground. To achieve this, data parsing and obstacle detection on the model are performed based on the IFC standard. Specifically, the spaces containing obstacles are divided using a prism-based partitioning approach. This methodology is illustrated using the example of turnstiles in a subway station using the following steps:

(1) Indoor vertex information is obtained from geometric point data of the IfcSpace class. Delaunay triangulation is performed on points with the same elevation, distributed by floor, extending upwards to the floor slabs, forming the edges of prismatic polyhedra.
(2) The turnstile devices are represented using simplified and minimal bounding boxes based on the semantic relationship information in IfcSpace. The bottom-left coordinate $(X_{\min}, Y_{\min}, Z_{\min})$ and top-right coordinate $(X_{\max}, Y_{\max}, Z_{\max})$ of the bounding box are calculated using the geometric information of obstacles.
(3) The subway turnstile and its surrounding space are represented by a vertical box in Fig. 4 The elevation value of the box, which includes the turnstile, is obtained based on semantic information, with a centroid value of $(Z_{IfcSpace} - Z_{IfcSpace-MMB})/2$. The 3D spatial segmentation results are shown in Fig. 5.

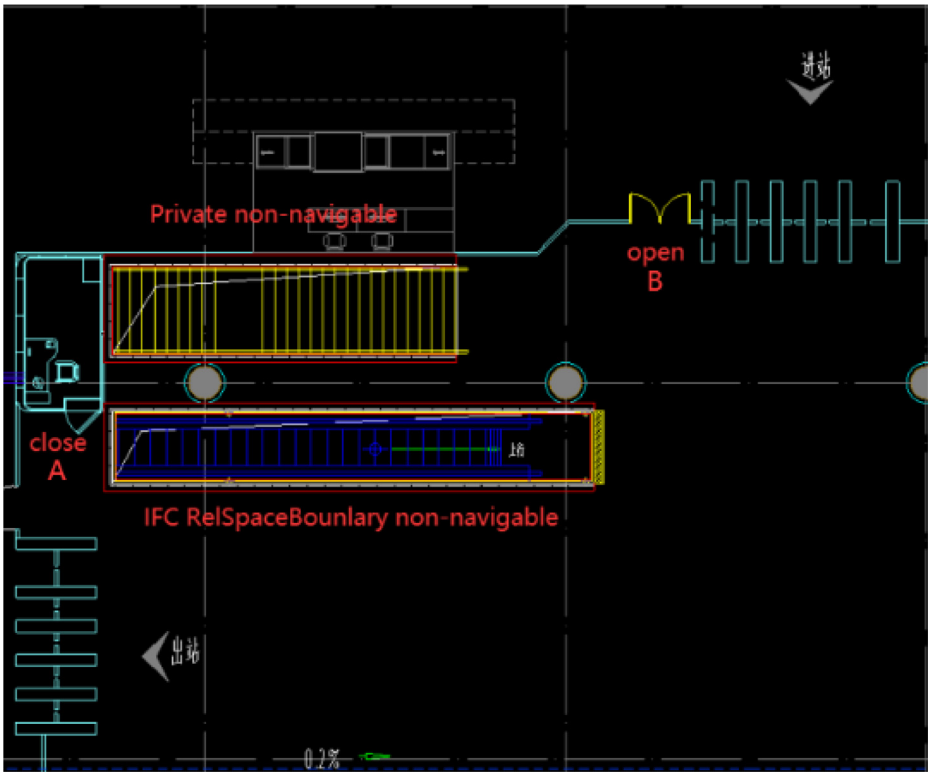

Fig. 2. CAD of part of Metro Square.

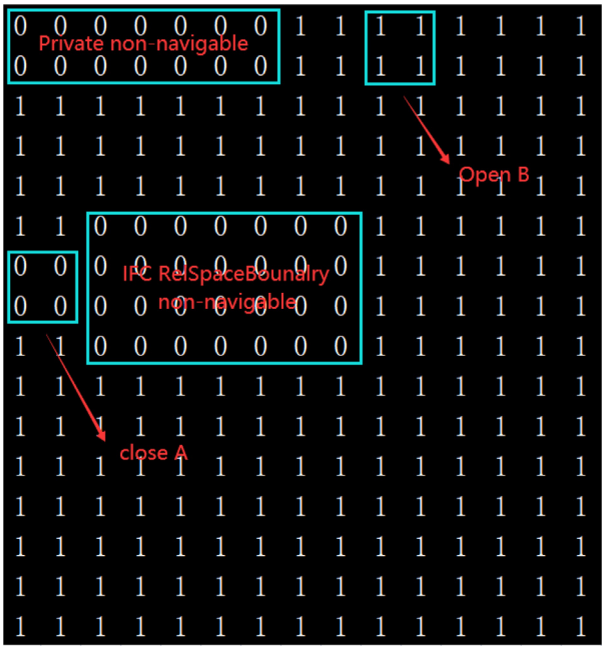

Fig. 3. Two-dimensional grid mapping diagram.

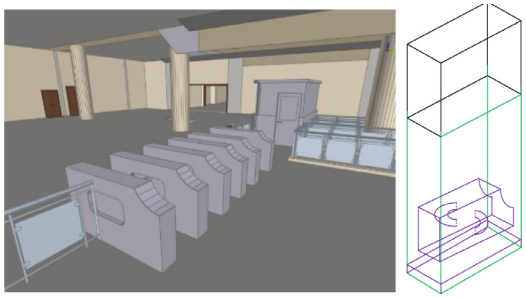

Fig. 4. Gate model and spatial outer box.

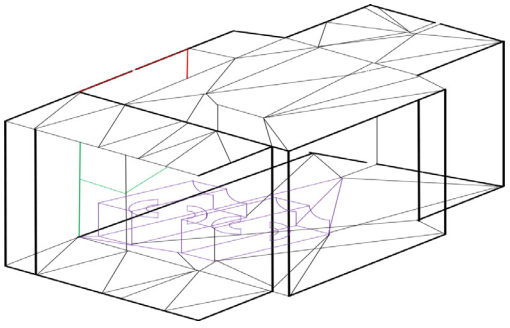

Fig. 5. 3D spatial sectioning results.

(4) The coordinates of the feature points in the spatial subspace of the partitioned points are determined based on the center point of the subspace. Specifically, the coordinates of the feature points within the vertical range of the turnstile box space are set as $((X_{\min} + X_{\max})/2, (Y_{\min} + Y_{\max})/2, (Z_{\min} + Z_{\max})/2)$.

(5) The feature points are connected to form an indoor navigable three-dimensional spatial region, which constitutes an indoor navigation road network. Figs. 6 and 7 show the comparison of the effect before and after the road network is divided. The black line is the navigation road network connected after mapping to the ground, while the triprism divided by the white line is the three-dimensional space area that can be used in navigation.

3.2. Indoor localization method based on BIM and AR

The positioning method based on BIM and AR primarily involves the design and installation of AR nodes. Through the detection, feature de-

Fig. 6. Map of the road network before subdivision.

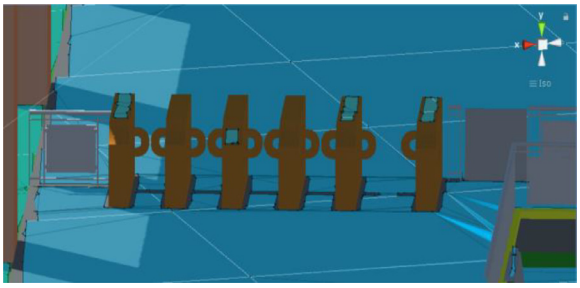

Fig. 7. Subdivided road map.

scription, and matching of AR nodes, as well as the estimation and tracking registration of the position and motion state of AR identification nodes, combined with camera coordinate transformation, the pedestrian position is computed to achieve indoor positioning. The method is mainly divided into three parts: camera calibration, rules for selecting AR nodes, and marker-based tracking registration technology.

3.2. 1 camera calibration

In the process of AR marking node matching, the known point coordinates and image point coordinates are used for camera calibration to determine the internal and external parameters of the smartphone camera to help determine the position and direction information of the marked nodes in the image (Paucher & Turk, 2010). Combined with the coordinate transformation relationship between the world coordinate system, Revit coordinate system, and camera coordinate system, the coordinates of AR marker nodes in the world coordinate system are obtained, and the coordinate correction is carried out by matching the BIM model and real-world nodes, in order to realize the indoor positioning of pedestrians.

The camera calibration process can determine the internal parameters and external parameters of the camera, determine the geometric characteristics and position relations of the camera, and then realize the transformation of the image coordinate system and the world coordinate system. In the process of camera calibration, the method proposed in the paper has the following requirements for the inherent parameters of the camera of the smartphone: the focal length of the camera is between 28 mm and 35 mm, which is suitable for a variety of shooting scenes; In order to provide good shooting results in different light conditions, the aperture range is between F/1.7 and F/2.4. Image sensors range in size from 1/2.55 inch to 1/1.7 inch and the resolution of the main camera ranges from 12 MP (megapixels) to 48 MP (megapixels). In addition, the smartphone also needs to have a monocular depth camera and gyroscope to support depth perception and attitude tracking in augmented reality applications. The camera's internal parameters remain fixed throughout the calibration process, using a calibration plate with known dimensions and geometric characteristics, using a linear calibration method as the initial estimate, and ignoring slight phone movement or shaking during shooting.

The world coordinate system determines the position and attitude of the measuring point in real space and is the reference coordinate system. The image coordinate system describes the position of pixels in the image. The camera coordinate system describes the position and orientation of the object in the image captured by the camera. Through the conversion between the world coordinate system, the image coordinate system, and the camera coordinate system, the combination of virtual and real scenes in the augmented reality system can be realized so as to realize AR navigation.

The conversion relationship between the image coordinate system and the camera coordinate system is shown in Eq. (1) :

$$Z_c\begin{bmatrix}x\\y\\1\end{bmatrix}=\begin{bmatrix}f&0&0&0\\0&f&0&0\\0&0&1&0\end{bmatrix}\begin{bmatrix}x_c\\y_c\\z_c\\1\end{bmatrix} \tag{1}$$

When using a wide-angle lens, there is a large distortion far from the center of the image. Nonlinear distortion can be described by the following formula:

$$\bar{x}=x+\delta_x(x,y) \tag{2}$$

$$\bar{y}=y+\delta_y(x,y) \tag{3}$$

In Eqs. (2) and (3), $\bar{x}$and $\bar{y}$are the ideal coordinates of the image points calculated by the pinhole linear model. (x,y) is the coordinate of the actual image point. δ_x and δ_y are the nonlinear distortion value, which is related to the position of the image point in the image, and can be expressed as:

$$\delta_x(x,y)=k_1x(x^2+y^2)+\left[p_1(3x^2+y^2)+2p_2xy\right]+s_1\left(x^2+y^2\right) \tag{4}$$

$$\delta_x(x,y)=k_2x(x^2+y^2)+\left[p_2(3x^2+y^2)+2p_1xy\right]+s_2\left(x^2+y^2\right) \tag{5}$$

In Eqs. (4) and (5), The first term of δ_x and δ_y is called radial distortion, the second term is called tangential distortion, and the third term is called thin prism distortion. k_1,k_2,p_1,p_2,s_1,s_2 are called the nonlinear distortion parameter.

Let the coordinates of a point in space in the world coordinate system and the camera coordinate system be (x_w,y_w,z_w) and (x_c,y_c,z_c), respectively, and the transformation relation is as follows:

$$\begin{bmatrix}x_c\\y_c\\z_c\end{bmatrix}=R\begin{bmatrix}x_w\\y_w\\z_w\end{bmatrix}+T \tag{6}$$

In Eq. (6), R is the rotation matrix and T is the three-dimensional translation vector. By combining (1) to (6), the relationship between the three-dimensional coordinates of the space point represented by the world coordinate system and the pixel coordinates of the corresponding projection point (u,v) can be obtained.

$$s\begin{bmatrix}u\\v\\1\end{bmatrix}=\begin{bmatrix}f/\Delta x&0&u_0&0\\0&f/\Delta y&v_0&0\\0&0&0&0\end{bmatrix}\begin{bmatrix}R&T\\0&1\end{bmatrix}\begin{bmatrix}x_w\\y_w\\z_w\\1\end{bmatrix}=M_1M_2X_W \tag{7}$$

In Eq. (7), M_1 is determined by f, Δx, Δy, u_0, v_0,because they only related to the internal parameters of the camera, so these parameters are called the internal parameters of the camera; M_2 is determined by the orientation of the camera with respect to the world coordinate system and is called the external parameter of the camera. Determining the internal parameters of the camera is called camera calibration.

The relative position of AR marker node image points in the world coordinate system and the linear model of the camera can be represented as follows:

$$s_i\begin{bmatrix}u_i\\v_i\\1\end{bmatrix}=\begin{bmatrix}m_{11}&m_{12}&m_{13}&m_{14}\\m_{21}&m_{22}&m_{23}&m_{24}\\m_{31}&m_{32}&m_{33}&m_{34}\end{bmatrix}\begin{bmatrix}x_w\\y_w\\z_w\\1\end{bmatrix} \tag{8}$$

In Eq. (8), $[u_i, v_i, 1]$ represents the homogeneous image coordinates, where u_i and v_i are the coordinates of the i th point on the image. m_{ij} denotes the i th row and j-th column element of the projection matrix M. $[x_{wi}, y_{wi}, z_{wi}, 1]$ represents the homogeneous world coordinates of the i th point on the AR marker. By solving for the camera's intrinsic parameter relationship (Eq. (9)), we can obtain:

$$m_{34}\begin{bmatrix} m_1^{\mathrm{T}} & m_{14} \\ m_2^{\mathrm{T}} & m_{24} \\ m_3^{\mathrm{T}} & 1 \end{bmatrix} = \begin{bmatrix} \alpha_x r_1^{\mathrm{T}} + u_0 r_3^{\mathrm{T}} & \alpha_x t_x + u_0 t_z \\ \alpha_y r_2^{\mathrm{T}} + v_0 r_3^{\mathrm{T}} & \alpha_y t_y + v_0 r_z \\ r_3^{\mathrm{T}} & t_z \end{bmatrix} \tag{9}$$

In Eq. (9), $m_i^T (i = 1, 2, 3)$is a row vector composed of the first three elements of the i th row of the matrix obtained using Eq. (9). m_i^4represents the element at the i th row and 4th column of matrix M. $r_i^T (i = 1, 2, 3)$represents the i th row of the rotation matrix R.

By comparing both sides of Eq. (9), it can be deduced that $m_{34}m_3 = r_3$. And since r_3 is the third row in the orthogonal identity matrix, obtaining $|r_3| = 1$, then $m_{34}|m_3| = 1$and $m_{34} = \frac{1}{|m_3|}$, r_3, u_0, v_0, a_x, a_ycan be derived and calculated from Eq. (10) to (14):

$$r_3 = m_{34}m_3 \tag{10}$$

$$\alpha_x = m_{34}^2|m_1 \times m_3| \; \alpha_y = m_{34}^2|m_2 \times m_3| \tag{11}$$

$$u_0 = (\alpha_x r_1^{\mathrm{T}} + u_0 r_3^{\mathrm{T}})r_3 = m_{34}^2 m_1^{\mathrm{T}} m_3 \tag{12}$$

$$v_0 = (\alpha_y r_2^{\mathrm{T}} + v_0 r_3^{\mathrm{T}})r_3 = m_{34}^2 m_2^{\mathrm{T}} m_3 \tag{13}$$

$$\alpha_y = m_{34}^2|m_2 \times m_3| \tag{14}$$

After camera calibration, Neges et al. (2017) identified and matched AR-tagged nodes according to vision sensor technology in AR, obtained node information, and combined inertial navigation technology for environmental positioning (Xu, Liu & Li, 2021). In order to overcome the problem of coordinate deviation caused by continuous use of inertial navigation sensors, the coordinate system of AR software Revit is introduced. Through transforming between the world coordinate system and Revit coordinate system, the matching of AR marker nodes in the world coordinate system and Revit coordinate system is achieved, the user's position coordinates are corrected, and indoor positioning based on BIM and AR technology is realized.

The transformation relationship between the Revit coordinate system and the world coordinate system is as follows:

$$\begin{bmatrix} x_a \\ y_a \\ z_a \end{bmatrix} = M\begin{bmatrix} x_b \\ y_b \\ z_b \end{bmatrix} + N \tag{15}$$

In the Eq. (15), (x_a,y_a,z_a)and (x_b,y_b,z_b)are the coordinate points in the world coordinate system and Revit coordinate system, M is the rotation matrix and N is the three-dimensional translation vector.

The essence of using AR technology for indoor navigation is to superimpose computer-generated navigation information (including text, images, 3D objects, etc.) into the real scene through visual fusion. In order to realize the user's positioning in the building BIM model, this paper adopts the identity-based tracking registration technology, realizes the registration method of the camera and virtual information location, and obtains the AR node coordinates.

3.2.2. AR node selection rules

During the construction of the indoor navigation network, the indoor area is divided into navigable areas and non-navigable areas. Users identify nodes with smartphones to achieve indoor positioning, and when the navigation path length is certain, they tend to plan the route through the AR node.

In order to make the navigation path more in line with the travel needs of pedestrians, under the balance of factors such as path distance, the selection of AR nodes should comprehensively meet the walking habits of indoor pedestrians and the visibility rules of signs and be as close as possible to the area of interest of pedestrians. Reasonable AR node Settings can reduce network costs and improve navigation efficiency. The selection rules of AR identification nodes are as follows:

1. Nodes can be regarded as escape channel signs. Considering that it is difficult for the camera to identify images through obstacles such as walls, in order to ensure that the nodes are within the visible range, it is necessary to process the AR identification nodes for visible traffic connection during the construction of the road network.
2. The smaller the Angle between the relative position direction of the node and the path, the easier the pedestrian can identify the node, and the higher the utilization rate.
3. The greater the visibility of the node, the higher the utilization. The visibility threshold R is used as the radius to establish the visible area of the node, and the road network path covered by the visible area occupies a large weight in the navigation algorithm.
   As shown in Fig. 8, the intersection point between the visible range of AR marking node and the road network is $S_1, S_2, S_3, S_4, S_5, S_6$. The length of the road network path covered by the visible range of AR marking node is calculated. When conducting indoor navigation, the road network path in the visible area of AR marking node is given a large weight.
4. The smaller the Angle with the path direction, the higher the utilization.

As shown in Fig. 9, taking a path from point O to point E in the road network as an example, the visual range of OE and AR identification node S_1, S_2 intersect at F,G,H and I. Among them, the length of path OA covered by the visual range of AR recognition node S_1 is FA, and the angle between path OA and AR recognition node is α_1. The length of path AB covered by the visual range of AR recognition node S_1 is AG, and the angle is α_2.The length of the path BC covered by the visual range of the AR recognition node S_2 is HI.The angle α_3 between the path BC and the AR recognition node.

The AR recognition node utilization of the defined path is

$$U(i)\begin{cases} \frac{\alpha}{S}, \; S > 0 \\ 0, \; else \end{cases} \tag{16}$$

In Eq. (16), $\alpha$is the Angle between the path direction and the AR identification node; S is the ratio of paths covered by the visual range of AR identifying nodes. In indoor navigation, the path obtained by path planning according to the road network is composed of road segments, so the AR node utilization rate of the navigation path can be obtained as follows.

$$R_{U(n)} = \sum_{i=1}^{n} U(i) \tag{17}$$

The smaller the value ofR_U, the higher the node utilization rate. In the Fig. 9, $\alpha_1 < \alpha_3 < 90°$, $\alpha_2 > 90°$, so it is easier for pedestrians to discover node S_1 in path OA than node S_2 in path BC; that is, the effective utilization time of node S_1 is longer. Therefore, when the path distance is the same and the nodes' visual ranges do not cover each other, the node utilization of path $O-A-F-C-D-E$ is higher than that of path $O-G-B-C-D-E$.

3.2.3. Identification based tracking registration technology

The BIM model visualizes the physical and functional characteristics of real buildings. In the construction of an indoor navigation network, AR nodes are established in the real road network as images that can be taken by smartphones. After the placement position of AR nodes is designed, these nodes correspond to the node positions in the real world and the node positions in the BIM model, thus establishing the

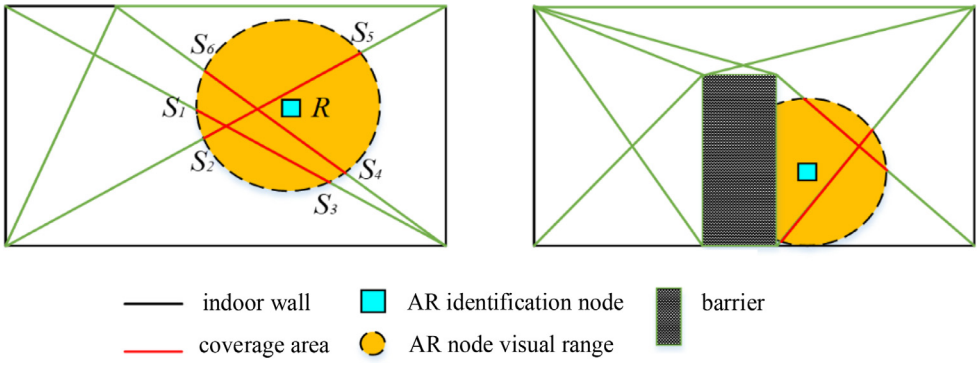

Fig. 8. Schematic diagram of AR identification node and pass connection.

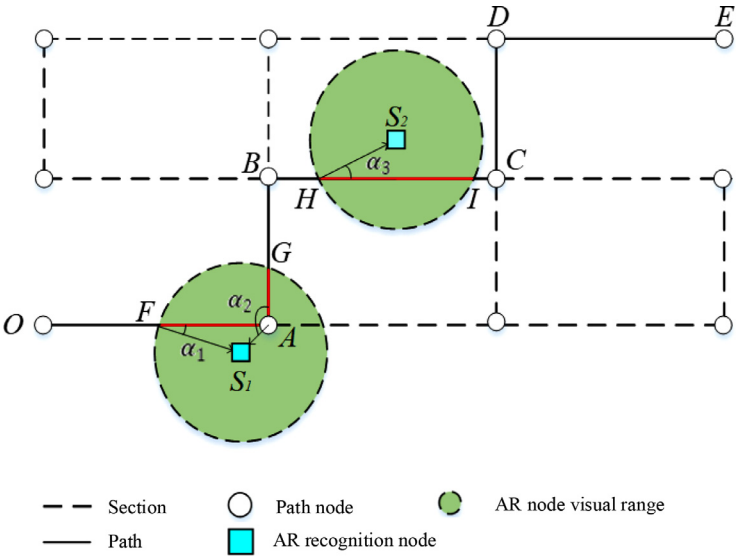

Fig. 9. Path AR node utilization.

AR marker node library. Through the identification of nodes, the corresponding relationship between nodes and the navigation network in the real world can be realized. In this paper, with the help of smartphones, identification-based tracking and registration technology is used to analyze and process the collected image or video data, and realize the detection of AR marker nodes, the feature description and matching of AR marker nodes, and the estimation and tracking registration of the position and motion state of AR marker nodes. Inertial navigation technology is used to fuse and process sensor data such as acceleration and angular speed to realize the position and direction information of smartphones and the indoor positioning of pedestrians.

The steps for feature extraction and coding recognition of identification nodes are as follows:

1) The image is binarized, and the simplified image is numerically calibrated to obtain the connected domain.
2) The boundary calibration algorithm is used to find the boundary of the region.
3) The homograph image transformation is used to find the corresponding pixel points bounded by the region boundaries.
4) The cross-correlation value between the captured photos and the AR node library images is calculated and compared with the specified threshold. The features are matched one by one between the inner pattern of the image and the mark point map in the established AR mark node library. Find the most interrelated mark images and realize AR mark nodes' tracking registration and recognition. The formula for calculating the cross-correlation between two images is:

$$\rho = \frac{\sum_x \sum_y (I(x,y) - \mu_1)(P(x,y) - \mu_P)}{\sigma_1 \rho_P} \tag{18}$$

In Eq. (18), $I(x,y)$and$P(x,y)$ represent the collected image and the matching template image, respectively. The mean and standard deviation of the calculated image are as follows:

$$\mu_1 = \frac{1}{xy}\sum_x \sum_y I(x,y),\ p = \frac{1}{xy}\sum_x \sum_y P(x,y) \tag{19}$$

$$\sigma_1 = \left(\sum_x \sum_y \left(I(x,y) - \mu_1\right)\right)^{\frac{1}{2}}, \sigma_P = \left(\sum_x \sum_y \left(P(x,y) - \mu_P\right)\right)^{\frac{1}{2}} \tag{20}$$

For each candidate identifier in the image, the image with the greatest correlation is found in the AR identification node library. If the cross-correlation value is greater than the specified threshold, the candidate identifier in the image is regarded as the corresponding identifier in the AR identification node library, and the decoding process is completed to realize the tracking registration and identification of the AR identification node.

In the detection and recognition process of AR tag nodes, FAST (Features from Accelerated Segment Test) is adopted as the detection algorithm of the tag nodes. The detected tag nodes are described in the AR-tag nodes' feature description and matching process and matched with the pre-stored identity node template to determine their position and attitude in the scene. In the estimation and Tracking registration process of AR identification node position and motion state, the optical flow tracking method KLT (Kanade Lucas Tomasi Tracking) is adopted to track the position changes of identification nodes in continuous image frames and the attitude between the camera and the real scene is

estimated according to the tracked information. Implement the tracking and registration of identification nodes.

3.3. Indoor augmented reality navigation algorithm

Based on the indoor road network constructed in Section 3.1 and the indoor positioning method based on AR node recognition described in Section 3.2, the location information of pedestrians in the building and the target position of pedestrians are obtained. This section proposes an indoor navigation path planning algorithm that combines the map information of the indoor road network, creates the optimal navigation path in the indoor road network, and displays the path on the mobile phone screen of pedestrians so as to realize indoor navigation. Indoor navigation path algorithms usually aim to obtain the shortest path or minimize the time or cost of the path. This paper takes into account the actual needs and walking preferences of pedestrians, who tend to choose routes that are less crowded, have wide views, have good light and ventilation, and are attracted by iconic places such as shops and restaurants, choose routes that provide quality facilities and services, more access to seats or elevators, toilets, toilets, etc. Water fountains and other necessary service locations (Vanclooster, van de Weghe & de Maeyer, 2016).

In the indoor navigation path optimization algorithm, the ant colony algorithm is prone to fall into the local optimal problem with less information in the early stage of routing. In this study, combined with the actual demand for indoor navigation, IFC model data and indoor road network structure are taken as the initial pheromones, and factors such as the utilization rate of AR recognition nodes, the number of AR nodes, and path distance are taken into account to improve ant colony algorithm. The IARA algorithm based on BIM and AR technology is proposed, in which the heuristic function and pheromone update method are optimized as follows:

Create a candidate solution set of path nodes. When the set of next selectable nodes of ant k contains node i, its probability P_i^k of selecting node i is as follows.

$$P_i^k = \begin{cases} \frac{[\tau_i(t)]^\alpha [\eta_i(t)]^\beta}{\sum [\tau_i(t)]^\alpha [\tau_i(t)]^\beta} & , i \in S_k \\ 0 & , else \end{cases} \tag{21}$$

In Eq. (21), α represents the parameter that limits the influence of$\tau_i(t)$, β represents the parameter that limits the influence of $\eta_i(t)$, while $\tau_i(t)$ and $\eta_i(t)$ represent the number of pheromones and the heuristic optimization function respectively when the node is at time t.

To reduce the angle between the path and the AR identification node, the angle between the current section direction and the next path direction leading to the end point is selected as the heuristic information. The heuristic function is set as follows.

$$\eta_i(t) = e^{\lambda \cos \omega} \tag{22}$$

In Eq. (22) λ denotes the parameter limiting the influence of ω.

The distance D of the road network navigation path should be defined. The AR of the path represents the node utilization R_U, and the number M of nodes is identified using AR. The single-objective solution V is defined, then:

$$\min(V) = \omega_1 \cdot D + \omega_2 \cdot R_U + \omega_3 \cdot M \tag{23}$$

In Eq. (23), ω_1,ω_2,$\omega_3$are the weights of the optimization objectives, and to represent the combined impact of multiple objectives, the above equation can be converted to:

$$\min(V') = \omega_1 \cdot \frac{D - D_{\min}}{D_{\max} - D_{\min}} + \omega_2 \cdot \frac{R - R_{U\min}}{R_{U\max} - R_{U\min}} + \omega_3 \cdot \frac{M - M_{\min}}{M_{\max} - M_{\min}} \tag{24}$$

In Eq. (24), $R_{U_{max}}$,D_{max} and M_{max} are the maximum values of R_U,D and M in the navigation area, respectively. $R_{U_{min}}$, D_{min}, M_{min} are the minimum values of D, R_U and M, respectively. The formula for updating pheromone of solution V' after unified dimension is

$$\tau_i(t+1) = (1-\rho)\tau_i + \Delta\tau_i^k(t) \tag{25}$$

$$\Delta\tau_i^k(t) = \begin{cases} \frac{Q}{V'}, else \\ 0, else \end{cases} \tag{26}$$

In Eqs. (25) and (26), Q is the total amount of pheromone, ρ is the rate of pheromone evaporation and $\rho \in [0, 1]$.

The steps of using IARA algorithm to solve the optimal path are as follows:

(1) Process semantic information and construct road network. According to the traffic rule constraints, the reachable tabu list of nodes is obtained.
(2) Initial setting, set the starting point ants number M, iteration times T, influence coefficient A and other parameters.
(3) After the iteration is completed, retrieve the endpoint ant and update the pheromone.
(4) Iterate until the limit is reached.
(5) Compare the results of each iteration until the path tends to be stable.

4. Implementation and results

4.1. Testing setting

This study uses JDK10+SDK+Android API 30 environment to write programs. Due to the application of AR technology, in order to obtain better AR navigation effect and route planning speed, it is recommended to use Android 11.0 or above system mobile phones. The depth camera, graphics camera, and motion tracking sensor must meet the following requirements: a Qualcomm Snapdragon 860 or later computing CPU, a ROM of >32 GB, sensors and gyroscopes that support motion tracking technology, and a single-eye depth camera.

This experiment took place in the subway square. Firstly, according to the setting rules of AR identification nodes proposed in Section 3.2.1, the AR nodes were designed and installed in the visible range so that the Angle between the node and the location direction and the path was small, and the node utilization rate was improved. 15 AR identification nodes are placed near subway entrances, platforms, information inquiry places, and other densely populated locations. Special tools and fixed devices are used to install the nodes to ensure their stability and durability. Each AR identification node is coded to correspond the location of the AR node to that of the real world.

Then, the identification based on tracking registration technology described in Section 3.2.3 is adopted to recognize and track the images. After the feature points of the identification nodes are identified and matched from the images collected by the camera, the identified nodes' position movement and movement are tracked, and the node position information is obtained in real-time. According to the camera's translation and rotation attitude in the subway square, the position and orientation of the camera in the subway square are calculated to realize the indoor positioning of pedestrians. Finally, the IARA path planning algorithm given in Section 3.3 is adopted to plan the pedestrian path in the road network map constructed in Section 3.1, and the planned navigation path is displayed in AR.

In the subway square, the map was abstracted into a grid navigation path map, and route planning was carried out, in which the black square represented obstacles, the blue square represented AR node positions, and the green circle and the red circle represented the starting point and the endpoint of the pedestrian respectively. Experiments and path analysis were conducted on indoor navigation path planning under the starting and ending points of three groups of subway squares: Table 2 is the algorithm parameters of IARA algorithm, Table 3 is the optimization

Table 2
IARA parameters.

Number of iterative ants	Maximum number of iterations	λ	α	β	ρ
10	20	0.5	0.5	5	0.2

Table 3
Regional optimization target parameters.

ω_1	ω_2	ω_3	$D_{\min}/m$	$R_{U_{\min}}$	$R_{U_{\min}}$	$R_{U_{\max}}$	$M_{\min}$	$M_{\max}$
2/5	2/5	2/5	0	300	0	300	0	10

Table 4
IARA algorithm navigation path results.

	Distance/m	Number of AR nodes	Node utilization/%
1	173	6	43
2	193	8	58
3	186	7	48

objective parameters of the experiment area, and the three optimization objectives were assigned the same weight.

4.2. Experimentation

In this study, the IARA algorithm and SPA algorithm are used as indoor navigation path planning algorithms for indoor navigation path planning. In the process of regional node navigation based on the IARA algorithm, the path nodes that have been visited but have not been expanded in the current candidate path are added to the OPEN table, and the CLOSED table stores the nodes that have been visited and will be visited or processed again. Start by adding the start node to the OPEN table and tracking the visited nodes through the CLOSED table. The start node that supports augmented reality navigation is added to the navigation sequence for each regional node. Then, under the condition that the OPEN table is not empty, each node is processed in a loop: the algorithm calculates the pheromone value of the node and checks whether the current node is an AR identifier node: for true, it is added to the optimal path sequence and jumps out of the loop; for false, the adjacent nodes of the current node are checked and processed accordingly, and the parent nodes and pheromone values are updated. Finally, the initial path is obtained step by step by adjusting the OPEN table.

When evaluating the performance of the path planning algorithm, we take the indoor navigation path distance, the utilization rate of AR recognition nodes, and the number of AR recognition nodes as evaluation criteria. The number of nodes passed by the path planned by the IARA algorithm and the node utilization rate are shown in Table 4.

Table 5
SPA algorithm navigation path results.

	Distance/m	Number of AR nodes	Node utilization/%
1	142	3	25
2	152	4	28
3	136	3	21

The application of the IARA algorithm to plan the path is shown in Fig. 10 with the yellow line, which can stably realize the indoor navigation of pedestrians.

SPA (Shortest Path Algorithm) is an improved algorithm of the A* algorithm. It uses A heuristic function to evaluate the direction of search. The value of the heuristic function is equal to the sum of the straight distance from the current node to the goal node and the distance from the current node to the start node. SPA algorithm can greatly reduce the number of search nodes and improve the search efficiency. In indoor navigation and path planning, the SPA algorithm is a commonly used shortest path algorithm. The specific search process of the SPA algorithm is as follows:

(1) Divide the indoor space into several grids and establish a hierarchical grid map. Each grid node contains the location information of the grid and the distance information to other grids.
(2) Starting from the starting point, search the nearest grid level to find the shortest path from the starting point to that level.
(3) If the grid node in this level doesn't contain an endpoint, expand to the next level and continue the search.
(4) Repeat step 3 until you find the endpoint or search all grid layers.
(5) If an endpoint is found, return the shortest path from start to finish. Otherwise, it indicates that there is no feasible path.

The number of nodes passed by the path planned by the SPA algorithm and the utilization rate of nodes are shown in Table 5. The path of indoor navigation implemented by the SPA algorithm, in this case, is represented by a pink line in Fig. 10.

4.3. Results and discussion

It is based on BIM and AR technology. The construction of the subway square indoor road network and the indoor positioning of pedestrians through the identification of AR nodes are described above. This process can only be completed according to smartphones, without the need to add additional sensor equipment. In the process of the experiment, the IARA algorithm and SPA algorithm were used to plan the pedestrian path in the network diagram of Subway Square when the indoor road network and the pedestrian starting point and destination were known.

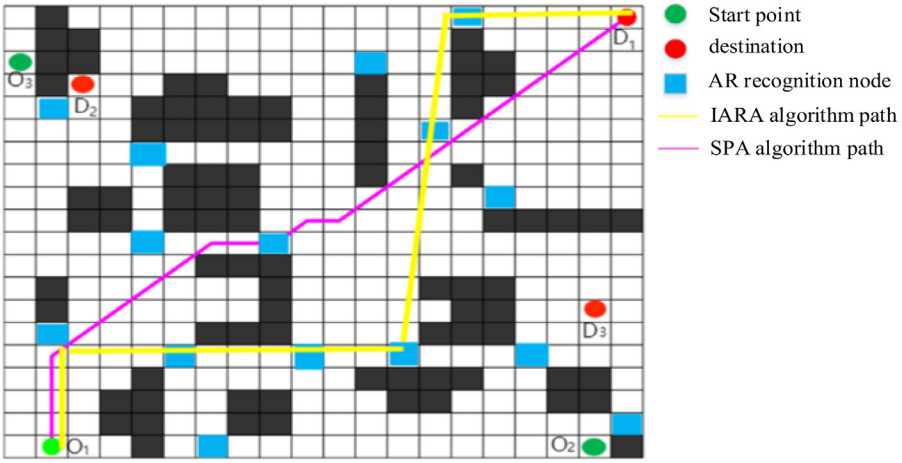

Fig. 10. Navigation path map.

Table 6
Comparison of navigation path results.

	Algorithm	Distance/m	Number of AR nodes	Node utilization/%
1	IARA	173	6	43
	SPA	142	3	25
2	IARA	193	8	58
	SPA	152	4	28
3	IARA	186	7	48
	SPA	136	3	21

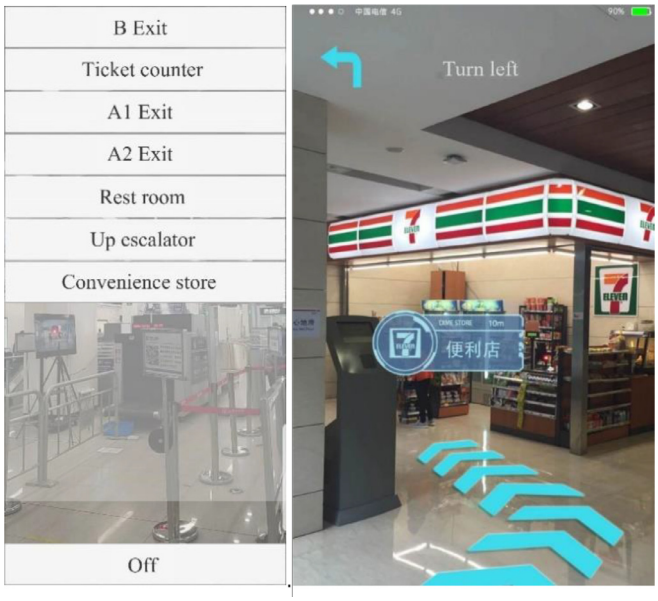

Fig. 11. AR navigation interface.

Both the IARA algorithm and the SPA algorithm can achieve the conclusion of indoor navigation path planning under constrained conditions. The path length, number of nodes, node utilization rate, and User Interest Coverage obtained by the two indoor navigation algorithms are shown in Table 6. The paths planned by the IARA algorithm and SPA algorithm in the metro square plane network diagram are represented as yellow lines and pink lines, respectively, in Fig. 10. As can be seen from the figure, the distance of the navigation path planned by the IARA algorithm is slightly longer than that planned by the SPA algorithm, but more AR nodes pass through, and the utilization rate of AR nodes is significantly higher. This shows that the route planned by the IARA algorithm makes it easier to reach important areas such as exits, and the route planned by the IARA algorithm is closer to the actual travel demand of pedestrians.

Fig. 11 takes the AR navigation function of the convenience store in the subway station as an example. In the navigation system, locations that may be of interest to nearby pedestrians and corresponding AR navigation routes can be displayed.

5. Conclusion

This paper proposes an indoor navigation method based on BIM and AR technology with the help of smartphones to realize indoor navigation more in line with the needs of pedestrians in the case of known building BIM models, geometric data, and semantic information. This method is divided into three parts: indoor navigation network construction, indoor pedestrian location and navigation path optimization algorithm, indoor navigation, and human-computer interaction. It only relies on smartphones, reasonably places AR identification nodes in indoor spaces, and does not attach sensors to realize indoor pedestrian positioning and indoor navigation. In the process of constructing the indoor road network, the spatial information of the three-dimensional model is subdivided into the two-dimensional plane through the triangular prism, and the indoor navigation network is constructed. Through camera calibration, coordinate system conversion, computer vision detection of AR nodes, and tracking registration of AR identification nodes, node information is obtained, and the information is analyzed by inertial navigation technology to determine the indoor location. Then, according to the proposed indoor augmented reality navigation algorithm based on architectural and spatial information, we plan routes for pedestrians in the indoor plane network. By comparing the routes planned by the IARA algorithm and the SPA algorithm, the path planned by the IARA algorithm passes through more AR identification nodes and has a higher node utilization rate. The superiority of the IARA algorithm is verified. Finally, an indoor navigation experiment based on BIM and AR is carried out in the subway square to verify the feasibility of the proposed method and its consistency with the travel needs of pedestrians.

Conflicts of interest

The authors declare that they have no conflicts of interest.

Data availability

The data used to support the findings of this study are available from the corresponding author upon request.

Acknowledgments

This study was supported in the form of funding by:
The Central Guidance for Local Science and Technology Development Fund Program of Hebei Province under Grant 246Z0802G, the Introducing Foreign Intelligence Program (2023-2025), the Shijiazhuang Science and Technology Planning Program under grant 236130217A, and the Shijiazhuang City Innovation Application Scenario Project (241130044A).

References

Agrawal, S., & Singh, S. (2014). Indoor localization based on bluetooth technology: A brief review. *International Journal of Computer Application, 97.8*, 31–33. 10.5120/17029-7327.

Alattas, A., Zlatanova, S., & van Oosterom, P. (2017). Supporting indoor navigation using access rights to spaces based on combined use of IndoorGML and LADM models. *ISPRS International Journal of Geo-information, 6.12*, 384. 10.3390/ijgi6120384.

Alqahtani, E. J., Alshamrani, F. H., & Syed, H. F. (2018). Survey on algorithms and techniques for indoor navigation systems. In *2018 21st Saudi Computer Society National Computer Conference (NCC)* (pp. 1–9). IEEE. 10.1109/ncg.2018.8593096.

Bai, X., Huang, M., & Prasad, N. R. (2019). A survey of image-based indoor localization using deep learning. In *2019 22nd International Symposium on Wireless Personal Multimedia Communications (WPMC)* (pp. 1–6). IEEE. 10.1109/wpmc48795.2019.9096144.

Bargh, M. S., & de Groote, R. (2008). Indoor localization based on response rate of bluetooth inquiries. In *Proceedings of the first ACM international workshop on Mobile entity localization and tracking in GPS-less environments* (pp. 49–54). 10.1145/1410012.1410024.

Bernardini, G., Lovreglio, R., & Quagliarini, E. (2023). Can active and passive wayfinding systems support fire evacuation in buildings? Insights from a virtual reality-based experiment. *Journal of Building Engineering, 74*, Article 106778. 10.1016/j.jobe.2023.106778.

Blunck, H., Godsk, T., & Grønbæk, K. (2010). PerPos: A platform providing cloud services for pervasive positioning. In *Proceedings of the 1st International Conference and Exhibition on Computing for Geospatial Research & Application* (pp. 1–8). 10.1145/1823854.1823869.

Chen, Z., Zhu, Q., & Jiang, H. (2015). Indoor localization using smartphone sensors and iBeacons. In *2015 IEEE 10th conference on industrial electronics and applications (ICIEA)* (pp. 1723–1728). IEEE. 10.1109/iciea.2015.7334389.

de Oliveira, L. C., Andrade, A. O., & de Oliveira, E. C. (2017). Indoor navigation with mobile augmented reality and beacon technology for wheelchair users. In *2017 IEEE EMBS International Conference on Biomedical & Health Informatics (BHI)* (pp. 37–40). IEEE. 10.1109/bhi.2017.7897199.

Dong, J., Xiao, Y., & Noreikis, M. (2015). iMoon: Using smartphones for image-based indoor navigation. In *Proceedings of the 13th ACM Conference on Embedded Networked Sensor Systems* (pp. 85–97). 10.1145/2809695.2809722.

El-Sheimy, N., & Li, Y. (2021). Indoor navigation: State of the art and future trends. *Satellite Navigation, 2.1*, 7. 10.1186/s43020-021-00041-3.

Fu, X., Zhang, H., & Wang, P. (2021). Automatic Construction of Indoor 3D navigation graph from crowdsourcing trajectories. *ISPRS International Journal of Geo-Information, 10.3*, 146. 10.3390/ijgi10030146.

Grejner-Brzezinska, D. A., Toth, C. K., & Markiel, J. N. (2009). Personal navigation: Extending mobile mapping technologies into indoor environments. *Boletim De Ciencias Geodesicas, 15.5*, 790–806. 10.1007/978-3-642-20338-1_120.

Haas, H., Yin, L., Wang, Y., & Chen, C. (2016). What is Lifi? *Journal of Lightwave Technology, 34.6*, 1533–1544. 10.1109/JLT.2015.2510021.

Harle, R. (2013). A survey of indoor inertial positioning systems for pedestrians. *IEEE Communications Surveys & Tutorials, 15.3*, 1281–1293. 10.1109/surv.2012.121912.00075.

He, S., & Chan, S. H. G. (2015). Wi-Fi fingerprint-based indoor positioning: Recent advances and comparisons. *IEEE Communications Surveys & Tutorials, 18.1*, 466–490. 10.1109/comst.2015.2464084.

Hsieh, C. H., Chen, J. Y., & Nien, B. H. (2019). Deep learning-based indoor localization using received signal strength and channel state information. *IEEE Access : Practical Innovations, Open Solutions, 7*, 33256–33267. 10.1109/access.2019.2903487.

Hu, Y., Liao, X., & Lu, Q. (2016). A segment-based fusion algorithm of WiFi fingerprinting and pedestrian dead reckoning. In *2016 IEEE/CIC International Conference on Communications in China (ICCC)* (pp. 1–6). IEEE. 10.1109/icchina.2016.7636828.

Jamali, A., Abdul-Rahman, A., & Boguslawski, P. (2017). An automated 3D modeling of topological indoor navigation network. *GeoJournal, 82*, 157–170. 10.1007/s10708-015-9675-x.

Kim, J., & Jun, H. (2008). Vision-based location positioning using augmented reality for indoor navigation. *IEEE Transactions on Consumer Electronics, 54.3*, 954–962. 10.1109/tce.2008.4637573.

Kim, J. S., Yoo, S. J., & Li, K. J. (2014). Integrating IndoorGML and CityGML for Indoor Space. *Web and Wireless Geographical Information Systems* W2GIS 2014. 10.1007/978-3-642-55334-9_12.

Laakso, M., & Kiviniemi, A. O. (2012). The IFC standard: A review of history, development, and standardization, information technology. *Itcon, 17.9*, 134–161. 10.3390/buildings6010007.

Li, A., Cao, J., & Li, S. (2022). Map construction and path planning method for a mobile robot based on multi-sensor information fusion. *Applied Sciences, 12.6*, 2913. 10.3390/app12062913.

Li, H., Men, Y., & Mao, H. (2023). Automatic generation of road network model for indoor floor plan navigation. In *3rd International Conference on Internet of Things and Smart City (IoTSC 2023). 12708* (pp. 78–83). 10.1117/12.2684042.

Li, Y., Park, J. H., & Shin, B. S. (2017). A shortest path planning algorithm for cloud computing environment based on multi-access point topology analysis for complex indoor spaces. *The Journal of Supercomputing, 73*, 2867–2880. 10.1007/s11227-016-1650-x.

Li, Y., Zhang, Y., & Pan, X. (2022). BIM-based determination of indoor navigation sign layout using hybrid simulation and optimization. *Automation in Construction, 139*, Article 104243. 10.1016/j.autcon.2022.104243.

Liu, J., Luo, J., & Hou, J. (2020). A BIM based hybrid 3D indoor map model for indoor positioning and navigation. *ISPRS International Journal of Geo-Information, 9.12*, 747. 10.3390/ijgi9120747.

Liu, Y., & Sun, Y. (2012). Mobile robot instant indoor map building and localization using 2D laser scanning data. In *2012 International Conference on System Science and Engineering (ICSSE)* (pp. 339–344). IEEE. 10.1109/icsse.2012.6257203.

Lovreglio, R., & Kinateder, M. (2020). Augmented reality for pedestrian evacuation research: Promises and limitations. *Safety Science, 128*, Article 104750. 10.1016/j.ssci.2020.104750.

Macher, H., Landes, T., & Grussenmeyer, P. (2017). From point clouds to building information models: 3D semi-automatic reconstruction of indoors of existing buildings. *Applied Sciences, 7.10*, 1030. 10.3390/app7101030.

Mazhar, F., Khan, M. G., & Sällberg, B. (2017). Precise indoor positioning using UWB: A review of methods, algorithms and implementations. *Wireless Personal Communications, 97.3*, 4467–4491. 10.1007/s11277-017-4734-x.

Milgram, P., & Kishino, F. (1994). A taxonomy of mixed reality visual displays. *IEICE Transactions on Information and Systems, 77.12*, 1321–1329. 10.1587/transinf.e93.d.1329.

Morar, A., Moldoveanu, A., & Mocanu, I. (2020). A comprehensive survey of indoor localization methods based on computer vision. *Sensors, 20.9*, 2641. 10.3390/s20092641.

Neges, M., Koch, C., & König, M. (2017). Combining visual natural markers and IMU for improved AR based indoor navigation. *Advanced Engineering Informatics, 31*, 18–31. 10.1016/j.aei.2015.10.005.

Nikoohemat, S., Diakité, A. A., & Zlatanova, S. (2020). Indoor 3D reconstruction from point clouds for optimal routing in complex buildings to support disaster management. *Automation in Construction, 113*, Article 103109. 10.1016/j.autcon.2020.103109.

Ochmann, S., Vock, R., & Wessel, R. (2016). Automatic reconstruction of parametric building models from indoor point clouds. *Computers & Graphics, 54*, 94–103. 10.1016/j.cag.2015.07.008.

Pala, M., Osati, N., & López-Colino, F. (2013). HCTNav: A path planning algorithm for low-cost autonomous robot navigation in indoor environments. *ISPRS International Journal of Geo-Information, 2.3*, 729–748. 10.3390/ijgi2030729.

Park, J. W., Cho, Y. K., & Martinez, D. (2016). A BIM and UWB integrated mobile robot navigation system for indoor position tracking applications. *Journal of Construction Engineering and Project Management, 6.2*, 30–39. 10.6106/jcepm.2016.6.2.030.

Paucher, R., & Turk, M. (2010). Location-based augmented reality on mobile phones. In *2010 IEEE Computer Society Conference on Computer Vision and Pattern Recognition-Workshops* (pp. 9–16). IEEE. 10.1109/cvprw.2010.5543249.

Riady, A., & Kusuma, G. P. (2022). Indoor positioning system using hybrid method of fingerprinting and pedestrian dead reckoning. *Journal of King Saud University-Computer and Information Sciences, 34.9*, 7101–7110. 10.1016/j.jksuci.2021.09.005.

Rizk, H., Elmogy, A., & Yamaguchi, H. (2022). A robust and accurate indoor localization using learning-based fusion of Wi-Fi RTT and RSSI. *Sensors, 22.7*, 2700. 10.3390/s22072700.

Sacks, R., Eastam, C., Lee, G., & Teichloz, P. (2018). *BIM handbook: A guide to building information modeling for owners, designers, engineers, contractors, and facility managers*. John Wiley & Sons.

Serra, A., Carboni, D., & Marotto, V. (2010). Indoor pedestrian navigation system using a modern smartphone. In *Proceedings of the 12th international conference on Human computer interaction with mobile devices and services* (pp. 397–398). 10.1145/1851600.1851683.

Subedi, S., & Pyun, J. Y. (2020). A survey of smartphone-based indoor positioning system using RF-based wireless technologies. *Sensors, 20.24*, 7230. 10.3390/s20247230.

Ta, V. C. (2017). Smartphone-based indoor positioning using Wi-Fi, inertial sensors and Bluetooth. *Université Grenoble Alpes; Hanoi University of sciences (Hanoi* 28-09. 10.1109/ipin.2018.8533809.

Teo, T. A., & Cho, K. H. (2016). BIM-oriented indoor network model for indoor and outdoor combined route planning. *Advanced Engineering Informatics, 30.3*, 268–282. 10.1016/j.aei.2016.04.007.

Topak, F., Pekericli, M. K., & Tanyer, A. M. (2018). Technological viability assessment of bluetooth low energy technology for indoor localization. *Journal of Computing in Civil Engineering, 32.5*, Article 04018034. 10.1061/(ASCE)CP.1943-5487.0000778.

van Bommel, W., & van Bommel, W. (2019). Light beyond illumination, interior lighting: Fundamentals. *Technology and Application*, 371–385. 10.1007/978-3-030-17195-7_15.

Vanclooster, A., van de Weghe, N., & de Maeyer, P. (2016). Integrating indoor and outdoor spaces for pedestrian navigation guidance: A review. *Transactions in GIS, 20.4*, 491–525. 10.1111/tgis.12178.

Wang, C. S. (2019). An AR mobile navigation system integrating indoor positioning and content recommendation service. *World Wide Web, 22.3*, 1241–1262. 10.1007/s11280-018-0580-3.

Xu, C., Liu, Z., & Li, Z. (2021). Robust visual-inertial navigation system for low precision sensors under indoor and outdoor environments. *Remote Sensing, 13.4*, 772. 10.3390/rs13040772.

Xu, M., Wei, S., & Zlatanova, S. (2017). BIM-based indoor path planning considering obstacles, ISPRS Annals of the Photogrammetry. *Remote Sensing and Spatial Information Sciences, 4*, 417–423. 10.5194/isprs-annals-iv-2-w4-417-2017.

Xu, Y., Wen, Z., & Zhang, X. (2015). Indoor optimal path planning based on Dijkstra Algorithm, International Conference on Materials Engineering and Information Technology Applications (MEITA 2015). *Atlantis Press*, 309–313. 10.2991/meita-15.2015.57.

Yan, J., Zlatanova, S., & Lee, J. B. (2021). Indoor traveling salesman problem (itsp) path planning. *ISPRS International Journal of Geo-Information, 10.9*, 616. 10.3390/ijgi10090616.

Yan, X., Liu, W., & Cui, X. (2015). Research and application of indoor guide based on mobile augmented reality system. In *2015 International Conference on Virtual Reality and Visualization (ICVRV)* (pp. 308–311). IEEE. 10.1109/icvrv.2015.48.

Yassin, A., Nasser, Y., & Awad, M. (2016). Recent advances in indoor localization: A survey on theoretical approaches and applications. *IEEE Communications Surveys & Tutorials, 19.2*, 1327–1346. 10.1109/comst.2016.2632427.

Zafari, F., Gkelias, A., & Leung, K. K. (2019). A survey of indoor localization systems and technologies. *IEEE Communications Surveys & Tutorials, 21.3*, 2568–2599. 10.1109/comst.2019.2911558.

Zhou, B., Zheng, T., & Huang, J. (2020). A pedestrian network construction system based on crowdsourced walking trajectories. *IEEE Internet of Things Journal, 8.9*, 7203–7213. 10.1109/jiot.2020.3038445.

Zhou, Y., Chen, H., & Huang, Y. (2018). An indoor route planning method with environment awareness. In *IGARSS 2018-2018 IEEE International Geoscience and Remote Sensing Symposium* (pp. 2906–2909). IEEE. 10.1109/igarss.2018.8518507.